Sec24C mediates a Golgi-independent trafficking pathway that is required for tonoplast localization of ABCC1 and ABCC2

Qiao-Yan Lv
Shanghai Institute of Plant Physiology and Ecology
Yi-Qun Gao
Shanghai Institute of Plant Physiology and Ecology
Ya-Ling Wang
National Key Laboratory of Plant Molecular Genetics, Institute of Plant Physiology and Ecology, Shanghai Institutes for Biological Sciences, Chinese Academy of Sciences, Shanghai 200032, China
Chu-Ying Zhang
Shanghai Institute of Plant Physiology and Ecology
Zhen-Fei Chao
Shanghai Institute of Plant Physiology and Ecology
Li-Yuan Zhong
Shanghai Institute of Plant Physiology and Ecology
Mei-Ling Han
Shanghai Institute of Plant Physiology and Ecology
Dai-Yin Chao (dychao@cemps.ac.cn)
Shanghai Institute of Plant Physiology and Ecology https://orcid.org/0000-0003-2832-4800

Article

Keywords: protein sorting, Golgi apparatus, Sec24C, ABCC1, ABCC2, Golgi-independent pathways

Posted Date: September 24th, 2020

DOI: https://doi.org/10.21203/rs.3.rs-74332/v1

Abstract

Protein sorting is an essential biological process in all organisms. Trafficking membrane proteins generally relies on the sorting machinery of the Golgi apparatus. However, many proteins have been found to be delivered to target locations via Golgi-independent pathways, but the mechanisms underlying this delivery system remain unknown. Here, we report that Sec24C, a component of coat protein complex II (COPII) vesicles, mediates the direct secretory trafficking of the phytochelatin transporters ABCC1 and ABCC2 from the endoplasmic reticulum (ER) to prevacuolar compartments (PVCs). After performing a genetic screening, we found that Sec24C loss-of-function mutants are hypersensitive to cadmium (Cd) and arsenic (As) treatments due to mislocalization of ABCC1 and ABCC2, which results in defects in the vacuole compartmentalization of the toxic metals. Further studies showed that Sec24C recognizes ABCC1 and ABCC2 through direct interactions to mediate their exit from the ER to PVCs in a Golgi-independent manner. These findings expand our understanding of Golgi-independent trafficking as well as COPII vesicles.

Introduction

Vacuoles, which are cellular membrane-bound organelles, are the largest compartments of plant cells, occupying up to 90% of the volume of cells. In plants, the vacuole is crucial for growth and development and has a variety of functions, including storage of ions and metabolites, waste recycling, intracellular environmental stability, and response to injury[1]. Implementation of these functions relies on transporters or other membrane proteins localized in the tonoplast.

Tonoplast proteins are synthesized in the endoplasmic reticulum (ER) and delivered to their destination via multiple routes[2–4]. A classic route that is highly similar to that in yeast and metazoans involves coat protein complex II (COPII)-mediated anterograde trafficking from the ER to the Golgi followed by traversing of the trans-Golgi network/early endosome (TGN/EE) to prevacuolar compartments (PVCs)/multivesicular bodies (MVBs) [5–7]. However, it has also been reported that some vacuolar proteins are delivered to the tonoplast, bypassing the Golgi[8]. Many cargoes and regulators in Golgi-dependent pathways have been identified[2–4]. In contrast, little is known about the molecular machinery mediating the direct ER-to-vacuole pathway.

In eukaryotes, the best-described mechanism of exiting the ER is via COPII-coated vesicles, which transport both membrane proteins and soluble cargoes to the cis-Golgi[9]. The COPII complex includes the small G-protein Sar1, a Sec23-Sec24 heterodimer and a Sec13–Sec31 heterotetramer[10–12]. Among these components, Sec24 functions as an adaptor to recognize the cargoes to be delivered. There are three Sec24 paralogues in *Arabidopsis thaliana* whose expression patterns are similar, but mutations of each paralogue result in distinct phenotypes. Mutations in Sec24A lead to lethal or severe protein trafficking defects are not complemented by overexpression of Sec24B or Sec24C[13, 14]. In contrast, only mild defects in gametogenesis were observed in the *sec24b* knock-out mutant and the *sec24b/sec24c* double

mutant[15], while there was no obvious defects observed in the *sec24c* loss-of-function mutant. These results suggest that different Sec24 paralogues are functionally diverse in terms of recognizing different protein cargoes or are even involved in distinct processes.

Compartmentalization is an essential process in plants to deal with toxic heavy metals which is dependent on a series of tonoplast transporters. Some tonoplast transporters, such as Heavy Metal ATPase 3 (HMA3)[16] and Natural Resistance Associated Macrophage Protein 4 (NRAMP4), are able to transport Cd^{2+} into or out of vacuoles[17,18], but the major transporters for vacuolar sequestration of heavy metals in *A. thaliana* are tonoplast-localized ATP-binding cassette transporters, namely, ABCC1 and ABCC2, which transport glutathione-conjugate complexes into plant vacuoles[19–21]. However, it is still unclear how the tonoplast localization of ABCC1 and ABCC2 is regulated.

In this study, we isolated a cadmium (Cd)- and arsenic (As)-hypersensitive mutant, *cas2*, which has a mutation in Sec24C. Our results show that the loss of function of Sec24C results in retention of ABCC1 and ABCC2 in the ER and thus defects in the vacuolar compartmentalization of heavy metals. Further studies showed that Sec24C directly binds to ABCC1 and ABCC2 and mediates their movement from the ER to PVCs through a Golgi-independent trafficking pathway. These findings help to elucidate the molecular mechanism regulating the Golgi-independent secretory pathway and broaden our conventional understanding of COPII.

Results

Sec24C does not affect Cd uptake or long-distance transport

A previous study showed that *Sec24C* is widely expressed in all tissues[15]. We confirmed this by expressing a β-glucuronidase (GUS) reporter driven by the native promoter of *Sec24C*, which exhibited signals in all examined tissues, but the signals were strongest in the roots (Extended Data Fig. 2a-e). We further examined whether *Sec24C* is inducible by Cd treatment by using quantitative reverse polymerase chain reaction and GUS reporter lines, and we found that its expression was stable during treatment (Extended Data Fig. 2f-h), supporting that Sec24C is constitutively expressed protein.

As *Sec24C* is expressed throughout the plant body, we wondered which tissue drives the Cd-sensitive phenotype of *cas2*. We thus performed a reciprocal grafting experiment involving wild-type and *cas2* plants. In terms of the primary root length, we found that the grafted plants with a *cas2* scion and wild-type roots were similar to the non-grafted or self-grafted wild-type plants when grown on media supplemented with 30 μM $CdCl_2$ (Extended Data Fig. 3a, b). However, the grafted plants with a wild-type scion and *cas2* roots were as sensitive to Cd as the non-grafted or self-grafted *cas2* plants were (Extended Data Fig. 3a, b). These data indicate that root expression of *Sec24C* determines the Cd sensitivity of roots. However, by using the fresh shoot weight to assess the Cd sensitivity of plants, we found that the expression of *Sec24C* in both the shoots and roots contributed to the Cd-sensitive phenotype, as the shoot weights of the grafted plants either with a *cas2* scion and wild-type roots or with

a wild-type scion and *cas2* roots were significantly lower than those of the wild-type controls during exposure to Cd (Extended Data Fig. 3c). Taken together, these data suggest that the Cd-sensitive phenotype caused by the mutation in *Sec24C* is not a simple result of defects in Cd uptake or long-distance transport.

To further investigate whether the Cd-sensitive phenotype of *cas2* was caused by defects in ion uptake or transport, we examined the Cd contents in roots, shoots, and xylem sap (Extended Data Fig. 3d-f). When the plants were grown in hydroponic media consisting of 20 μM $CdCl_2$, the root Cd content of *cas2* was similar to that of wild-type Col-0 (Extended Data Fig. 3d), while the shoot Cd content of *cas2* was slightly lower than that of Col-0 (Extended Data Fig. 3e). Moreover, there was no significant difference in xylem sap Cd content between *cas2* and Col-0, either when they were grown on normal soil or soil supplied with 20 μM Cd (Extended Data Fig. 3f). These data indicated that the Cd stress-sensitive phenotype of *cas2* is not a result of excessive Cd uptake or accumulation.

Sec24C is required for vacuolar sequestration of Cd

To examine whether Sec24C confers Cd tolerance by vacuolar sequestration of this non-essential element, the cellular distribution of Cd was examined in the wild type and the mutant by the use of a Cd indicator dye. Protoplasts were isolated from wild-type and *cas2* mutant plants grown on media in the presence or absence of 10 μM Cd for 2 weeks, after which they were loaded with a Cd-sensitive fluorescent probe, Leadmium™ Green[22]. In the absence of Cd, protoplasts from the wild-type and mutant plants showed a negligible Leadmium™ Green fluorescence signal (Fig. 3a, b). In contrast, strong green fluorescence was observed in the vacuole of the protoplasts isolated from the wild-type plants grown on media supplemented with 10 μM Cd (Fig. 3c); however, nearly all protoplast cells isolated from *cas2* grown on media containing 10 μM Cd exhibited a strong signal in the cytoplasm but a much weaker signal in the vacuole (Fig. 3d-f). These results indicate that the amount of Cd sequestered in the vacuole is markedly reduced in the *cas2* mutant.

To confirm the Cd indicator results, we further analysed the vacuolar Cd content via inductively coupled plasma mass spectrometry (ICP-MS). After the plants grew for three weeks under normal conditions and then for four days in a hydroponic solution consisting of 20 μM $CdCl_2$, vacuoles of wild type and *cas2* were isolated and their Cd contents were subsequently measured via ICP-MS. As expected, the vacuoles isolated from the mutant contained much less Cd than did those isolated from wild type (Figs. 1g, 3g). These results, together with those from the Cd indicator experiment, revealed that *Sec24C* is required for Cd compartmentalization in vacuoles.

Sec24C regulates tonoplast targeting of ABCC1 and ABCC2

Heavy metal compartmentalization is mediated by multiple tonoplast transporters; therefore, we hypothesized that some or all of these transporters require Sec24C for their tonoplast localization. To test this hypothesis, we examined the subcellular localization of several tonoplast transporters related to heavy metal compartmentalization by expressing them with a green fluorescent protein (GFP) tag in

protoplasts and in stable transgenic plants. NRAMP3 and NRAMP4, two transporters involved in mobilizing the export of divalent cationic metals from vacuoles[17, 18], were first examined. According to the GFP signals from the osmotically lysed protoplasts, NRAMP3-GFP or NRAMP4-GFP was observed to be localized on the tonoplast either in Col-0 or *cas2* (Extended Data Fig. 4a, c, g, i). These results were further confirmed through observations of root cells of the transgenic Col-0 and *cas2* mutant lines stably and heritably expressing a NRAMP3-GFP or NRAMP4-GFP chimeric protein (Extended Data Fig. 4b, d, h, j). Like NRAMP3 and NRAMP4, HMA3, which sequesters Cd^{2+} into vacuoles, was also observed to be localized on tonoplasts in both Col-0 and *cas2* (Extended Data Fig. 4e, f, k, l). These data demonstrate that tonoplast localization of these three tonoplast transporters does not require Sec24C.

Though the ion forms of heavy metals such as Cd^{2+} can be directly transported into vacuoles, the major heavy metal detoxification strategy in plants involves metals or metalloids being sequestered into vacuoles in the form of glutathione-conjugate complexes, which is mediated by two ABC transporters, ABCC1 and ABCC2, in *A. thaliana*. We then focused on the subcellular localization of these two tonoplast transporters. As expected, both proteins were clearly localized to the tonoplast in Col-0, as revealed by their expression with a GFP tag in the protoplasts (Fig. 4a, e) and the stability and heritability of the transgenic lines (Fig. 4b, f). However, subcellular localizations of ABCC1 and ABCC2 clearly changed in *cas2*. Observations of the GFP signals either in root cortical cells or leaf pavement cells revealed that both ABCC1 and ABCC2 are entirely localized to the ER-like structure in *cas2* (Fig. 4d, h). Transient co-expression of GFP-tagged ABCC1 or ABCC2 with an ER marker in protoplasts isolated from *cas2* confirmed that ABCC1 and ABCC2 indeed accumulate in the ER of the mutant (Fig. 4c, g). These findings suggest that Sec24C plays a crucial role in the movement of ABCC1 and ABCC2 to the vacuolar membrane. These data indicate that Sec24C is required for the sorting of ABCC1 and ABCC2 during their existing from the ER.

To further confirm that Sec24C regulates heavy metal tolerance through ABCC1 and ABCC2, we analysed the genetic relationships of *Sec24C* with *ABCC1* and *ABCC2*. We isolated the *abcc1/abcc2* double mutant and generated *sec24c/abcc1/abcc2* triple mutant by crossing the double mutant with *sec24c-1* and screening the F2s. Our results revealed no significant difference among the different genotypes when grown on 1/2-strength Murashige and Skoog (MS) media (Fig. 4i, k). In contrast, when exposed to 30 μM $CdCl_2$, *sec24c-1*, *abcc1/abcc2* and *sec24c/abcc1/abcc2* were more sensitive to Cd than Col-0 was; however, *sec24c-1* was the most sensitive, while the sensitivities of *abcc1/abcc2* and *sec24c/abcc1/abcc2* were similar (Fig. 4j, k). These data indicate that Sec24C acts upstream of ABCC1 and ABCC2 and suggest that ER localization of ABCC1 and ABCC2 probably leads to ER stress in *sec24c-1*.

Sec24C is able to bind ABCC1 and ABCC2

Sec24 functions as an adaptor to recognize cargoes in the COPII complex[23, 24], so we examined whether Sec24C is able to bind and recognize ABCC1 and ABCC2 in *A. thaliana*. We first performed bimolecular luciferase complementation (BiLC) experiments between Sec24C and the two ABCC transporters in

Nicotiana benthamiana leaves (Fig. 5a). We found that both Sec24C/ABCC1 and Sec24C/ABCC2 are able to restore the luciferase activity of the split LUC protein, indicating that Sec24C interacts with ABCC1 and ABCC2 individually. To further validate the interactions of ABCC1 and ABCC2 with Sec24C, we carried out yeast two-hybrid (Y2H) experiments by using a split ubiquitin-based membrane Y2H system (Clontech, Mountain View, CA, USA). The results showed that the NMY51 strain yeast cells co-transformed with pPR3-Sec24C together with the pBT3-ABCC1 or pBT3-ABCC2 construct were able to grow on selection media (Fig. 5c), confirming that both ABCC1 and ABCC2 are able to physically interact with Sec24C in vitro.

To demonstrate whether Sec24C also binds ABCC1 and ABCC2 in vivo, we also conducted bimolecular fluorescence complementation (BiFC) assays in *A. thaliana* mesophyll protoplasts (Fig. 5b). As expected, the fluorescence of yellow fluorescent protein (YFP) was observed in protoplasts co-expressing Sec24C-YFPN and ABCC1-YFPC or co-expressing Sec24C-YFPN and ABCC2-YFPC, while no yellow fluorescence was detected from the negative control (Fig. 5b), indicating that Sec24C is able to bind to ABCC1 and ABCC2 in vivo. To further confirm these findings, we also performed a co-immunoprecipitation (Co-IP) assay. We found that ABCC1 and ABCC2 co-immunoprecipitated with Sec24C, confirming the interactions of Sec24C with ABCC1 and ABCC2 (Fig. 5d, e). Taken together, these results revealed that Sec24C functions as an adaptor to bind and recognize ABCC1 and ABCC2 in vivo.

ER-to-tonoplast trafficking of ABCC1 is dependent on COPII but not the Golgi

The COPII complex mediates the trafficking of cargo proteins from the ER to the Golgi. As Sec24C is involved in the trafficking of ABCC1 and ABCC2, we hypothesized that the trafficking of these two transporters from the ER to the Golgi depends on the COPII complex. To test this, we examined the effects of overexpression of Sec12p, which inhibits assembly of COPII vesicles[25-27], on ABCC1 localization. We observed that Sec12 overexpression caused a dramatic retention of ABCC1-GFP in the ER compared with that in the control (Extended Data Fig. 5a, b), confirming that ABCC1 exits the ER in a COPII-dependent manner.

To further determine the trafficking route of ABCC1, we treated the roots of Col-0 expressing ABCC1-GFP with brefeldin A (BFA), an inhibitor of Golgi and post-Golgi endomembrane trafficking; this inhibition leads to the formation of a BFA compartment comprising the Golgi, TGN, and endosome aggregates[28, 29]. Surprisingly, ABCC1-GFP was not detected in the BFA bodies as indicated by FM4-64 after 2 hours of BFA treatment (Fig. 6c, d), indicating that trafficking of ABCC1 from the ER to the tonoplast is independent of the Golgi. To confirm this, we further treated the plants with concanamycin A (ConcA)[30], a chemical that causes aggregation of the TGN/EE (Fig. 6e, f). The results showed that the membrane tracer FM4-64 aggregated and blocked tonoplasts at 2 hours after ConcA treatment, while ABCC1-GFP was not found in the aggregated compartments, further confirming that the ER-to-tonoplast trafficking of ABCC1 bypasses the Golgi and post-Golgi processes.

Sec24C mediates the movement of ABCC1 from the ER to PVCs

Given that the COPII complex is believed to function in protein sorting from the ER to the Golgi, the trafficking route of ABCC1 bypassing the Golgi raises the interesting question of how Sec24C mediates the tonoplast localization of ABCC1 after the protein exits the ER. The subcellular localization of Sec24C was previously evaluated at the ER-Golgi interface, the so-called ER exit site (ERES)[15], as it is close to the Golgi. We repeated this experiment in a previous study by co-expressing fusion proteins of Sec24C-GFP and SYP31-mCherry in *A. thaliana* leaf epidermal cells. We indeed noticed that some of the punctate structures labelled by Sec24C-GFP are close to the Golgi, as indicated by SYP31-mCherry, but most of the structures were separated from the Golgi (Fig. 7a). To confirm these findings, we co-expressed another Golgi marker, ST-mCherry, together with Sec24C-GFP in *A. thaliana* mesophyll protoplasts (Fig. 7b). We consistently observed that the co-localization of Sec24C-GFP and ST-mCherry was quite low (Fig. 7b, c). These data suggest that Sec24C probably localizes mainly in other vesicles.

As Sec24C mediates a Golgi-independent trafficking route from the ER to the vacuole, we wondered whether Sec24C localizes in PVCs to mediate ABCC1 trafficking directly from the ER to the PVCs. To address this question, we co-expressed Sec24C-GFP with the PVC marker RFP-Rha1[31] in *A. thaliana* mesophyll protoplasts (Fig. 7d). Interestingly, Sec24C-GFP indeed highly co-localized together with RFP-Rha1 (Fig. 7d, e), indicating that Sec24C is able to localize in PVCs. Moreover, we also co-expressed Sec24C-GFP together with another PVC marker, RFP-Ara7[32], the results of which further confirmed the localization of Sec24C in PVCs (Fig. 7f, g). These data demonstrate that Sec24C may mediate the direct trafficking of ABCC1 from the ER to PVCs. The BiFC experiment confirming the interactions of Sec24C with ABCC1 and ABCC2 also revealed a punctate structure at the interaction site (Fig. 5b). If Sec24C mediates trafficking of ABCC1 and ABCC2 directly from the ER to PVCs, Sec24C must colocalize together with ABCC1 and ABCC2 in the PVCs. To test this hypothesis, we reperformed our BiFC experiment with the addition of the PVC marker RFP-Rha1 (Fig. 7h-k). The results showed that the interaction site of Sec24C and ABCC1 overlapped with the PVCs, indicating that Sec24 mediates direct ABCC1 trafficking from the ER to the PVCs.

Discussion

Integral membrane proteins of lysosomes in animal cells, of tonoplasts in plant cells, and of vacuoles in yeast follow similar secretory pathways[33], in which cargoes are gathered into COPII vesicles for export from the ER and are transported to the destination membrane after being packaged into vesicles. There are many studies on the machinery of COPII in yeast; however, vacuolar protein sorting and transport is likely to be a more complex process in plants than in yeast, given that plants harbour genomes that are much more complex with respect to gene and genome duplication, which may be a result of natural selection, given that plants have to withstand harsh environmental conditions in a niche without any protection[34]. A unifying model has not yet been constructed on how many different routes mediate transport to the vacuoles. In this study, we employed a forward genetics-based approach to determine that Sec24C, a component of COPII, mediates a novel ER-PVC trafficking route that is indispensable for correct targeting of ABCC1 and ABCC2 to the tonoplast and confers heavy metal tolerance to *A. thaliana*.

Research on ABCC-type phytochelatin transporters in the past decade has focused predominantly on their function in vacuolar sequestration, which plays crucial roles in plants in response to heavy metal stress. However, the precise mechanisms that regulate ABCC1 and ABCC2 localization to tonoplasts remain poorly understood. This study showed that trafficking of these two transporters relies on a novel COPII-dependent and Golgi-independent pathway. As a component of COPII, Sec24C functions as an adaptor to recognize ABCC1 and ABCC2 through direct interaction. Loss of unction of Sec24C results in severe defects in ABCC1 and ABCC2 in the ER and thus causes a hypersensitive phenotype in response to heavy metal stresses. Interestingly, the *sec24c-1* single mutant exhibits a more severe phenotype than does the *abcc1/abcc2* double mutant and the *sec24c/abcc1/abcc2* triple mutant, demonstrating once again that the location of a protein is probably more important than its function.

Previous studies support the notion that different vacuolar cargoes are transported from the ER via multiple routes in plants[33, 35]. In many cases, the Golgi is an essential organelle for sorting these cargoes, but some evidence indicates the existence of Golgi-independent routes for unconventional vacuolar cargoes[8]. Elucidating the mechanisms underlying these processes are important not only for determining the function and regulation of cargo but also for understanding vesicle trafficking in general. This study showed that vacuolar cargoes such as ABCC1 and ABCC2 can be sorted at the ER-PVC interface, which expands our understanding of protein sorting. We show that Sec24C can bind and recognize ABCC1 and ABCC2 directly but that Sec24C is not required for other tonoplast proteins, such as NRAMP3, NRAMP4, and HMA3, indicating that the trafficking route selectivity of different cargoes is determined probably by the specificity of recognition by different Sec24 isoforms. However, the mechanism and motifs governing the recognition by Sec24C are still unclear. Identification of additional Sec24C-interacting proteins or identifying additional phenotypes of the *sec24c* mutants would help address this question.

In all eukaryotes, the best-described mechanism of ER exiting involves COPII-coated vesicles, which transport both membrane proteins and soluble cargoes to the Golgi. Various functions of COPII subunit paralogues exist in plants[36]. Five Sar1s, seven Sec23s, three Sec24s, two Sec13s, and two Sec31s have been identified in *A. thaliana*. However, whether different COPII subunit paralogue combinations constitute distinct carriers and whether differences in cargo-binding affinity occur between Sec24 paralogues remain unknown. Loss of function of *Sec24C* was previously found to have little impact on plant growth and development, which contrasts with the mild effects of mutations in *Sec24B* and the severe effects of mutation in *Sec24A*[13-15]. Given the expression patterns of these three genes, the different phenotypes of these mutants seemed to be explained only by their different recognition specificities, though their corresponding cargoes were totally unknown. The identification of ABCC1 and ABCC2 as target cargoes of Sec24C represents the first case of COPII recognition mechanisms in plants. In addition, we found that Sec24C localizes mainly in PVCs rather than in the ERES, as previously reported, which, together with other evidence, indicates that Sec24C is able to mediate direct ER-to-PVC trafficking of phytochelatin transporters.

In summary, this study identified a key regulator that is involved in the heavy metal stress tolerance of plants and that mediates the tonoplast localization of phytochelatin transporters through a previously unknown ER-to-PVC transferring route. These findings not only improve our understanding of protein-sorting mechanisms but also refresh our knowledge about the functional diversity of COPII.

Materials And Methods

Expression vector constructs

For *sec24c* complementation experiments, a genomic DNA fragment of *Sec24C* was obtained via PCR and was then recombined into a *pHMS* plant expression vector using a one-step PCR cloning kit. ABCC1/2-pHMS-GFP, NRAMP3/4-pHMS-GFP and HMA3-pHMS-GFP were cloned using the same strategy. The coding sequence without the stop codon of *Sec24C* was amplified from Col-0 cDNA and then inserted into a 35S-driven *pCAMBIA1300* OE vector to generate the Sec24C-1300 OE construct. To generate a *pSec24C*::*GUS* construct, a 2,199-bp fragment upstream of the *Sec24C* start codon was amplified via PCR from Arabidopsis genomic DNA (Col-0) and then introduced into a pCAMBIA1303 vector. GUS histochemical staining was performed as previously described[39]. For the constructs used for transient expression in Arabidopsis protoplasts, the cDNAs encoding the corresponding genes were amplified from Col-0, with the exception that *HMA3* was cloned from Arabidopsis ecotype Wassilewskija (Ws) and cloned into pA7 vectors modified to contain GFP and RFP under the 35S promoter by restriction digestion. For subcellular localization analysis in tobacco leaves, the cDNAs encoding the corresponding genes were cloned into *pCAMBIA1300* vectors modified to contain the mCherry sequence. For luciferase complementation imaging assays, coding sequences of *ABCC1*, *ABCC2* and *Sec24C* from the Col-0 cDNA were cloned into JW771 (N-terminal half of luciferase, NLUC) and JW772 (C-terminal half of luciferase, CLUC)[40], respectively, yielding ABCC1/2-NLUC and Sec24C-CLUC constructs, respectively, For Y2H analysis, the cDNAs were cloned into *pBT3-STE* and *pPR3-N* vectors. For BiFC assays, *ABCC1* and *ABCC2* were individually recombined into *pC131-YC* yielding *ABCC1-YFPC* and *ABCC2-YFPC*, respectively. *Sec24C* was recombined into *pC131-YN* yielding *Sec24C-YFPN*. The coding DNA sequences (CDSs) of *ABCC1/2* and *Sec24C* were independently fused to pHB-Myc and p1306-Flag vectors, respectively. All of the above constructs were verified by sequencing, and all of the primers used in this work are listed in the Supplementary Table 1.

Gene expression analysis

Total RNA was extracted from whole seedlings of 2-week-old Col-0 and *cas2* using TRIzol reagent (R0016; Beyotime, Shanghai, China) according to the manufacturer's instructions. The methods applied for real-time PCR were the same as those described in previous studies[37, 38]. RNAs from three batches of independently prepared plant materials (different plants constituted different biological replicates), each performed in triplicate (technical replications), were analysed. All of the primers used in this study are listed in the Supplementary Table 1.

A. thaliana grafting

Reciprocal grafting was performed as previously described[37, 38]. Healthy grafted plants without adventitious roots were transferred to media supplemented with Cd and grown in the same controlled environment as that described above. After 10 days, the seedlings on square dishes were visualized and photographed to assess their heavy metal tolerance.

Elemental analysis

Elements within *A. thaliana* leaf and root tissues were analysed via ICP-MS as previously described[37, 38]. The elements were analysed with an inductively coupled plasma mass spectrometer (NexION 350D; PerkinElmer, Waltham, MA) coupled to an Apex desolvation system and an SC-4 DX autosampler (Elemental Scientific Inc., Omaha, NE). All the samples were normalized with a heuristic algorithm using the best-measured elements as previously described[41].

Protoplast isolation, transformation, and osmotic lysis of plasma membranes

Protoplasts were isolated according to a previously reported protocol, with slight modifications[42]. The pelleted protoplasts were resuspended in MMG buffer (0.4 M mannitol, 15 mM $MgCl_2$ and 2 mM 2-(N-morpholino)ethanesulfonic acid (MES); pH 5.7, adjusted with KOH) by inverting the tubes.

With respect to the Cd-sensing fluorescent dye, protoplasts were isolated from two-week-old seedlings grown on 1/2-strength MS media in the presence or absence of Cd. The same number of protoplasts from the wild type and the mutant were incubated in 0.04% (v/v) Leadmium™ Green (Molecular Probes, Invitrogen) in MMG buffer at room temperature for 30 min in the dark. The protoplasts were stored on ice before microscopy observations. For transient expression, 200 microlitres of MMG/protoplast solution and 10 micrograms of the respective DNA construct were incubated together, after which the mixture and 220 microlitres of polyethylene glycol (PEG) buffer (40% PEG 4000, 0.8 M mannitol and 1 M $CaCl_2$) were then mixed together. After a 5-min incubation at room temperature, the mixture was diluted with 1 mL of W5 solution (154 mm NaCl, 125 mM $CaCl_2$, 5 mM KCl, 2 mM MES, adjusted to pH 5.7 with KOH). The protoplasts were centrifuged for 2 min at 100 × g, resuspended in 1 mL of W5 solution and centrifuged again. The protoplasts were subsequently suspended in 1 mL of WI solution (0.5 M mannitol, 20 mM KCl and 4 mM MES; pH 5.7, adjusted with KOH) and incubated overnight at 23 °C in the dark. After 24 hours, the protoplasts were monitored directly, or they and an equal volume of lysis buffer (200 mM sorbitol, 10% Ficoll, 20 mM EDTA, 10 mM hydroxyethyl piperazineethanesulfonic acid (HEPES); pH 8.0, adjusted with KOH) were mixed together to destabilize the plasma membranes and release the vacuoles.

Vacuole isolation

Vacuole isolation was carried out to measure the Cd content in the vacuoles of the wild type and *cas2* mutant. When they were 3 weeks old, the hydroponically grown seedlings were exposed to 0 (control) or 20 μM $CdCl_2$ (treatment) for 4 days. Afterward, 10 mL of pre-warmed (37 °C) 10% Ficoll buffer (0.2 M

mannitol, 10% Ficoll, 5 mM sodium phosphate, 10 mM EDTA; pH 8.0) was added to the pelleted protoplasts, which were then transferred the lysed protoplast solution. After 2 min of incubation, the samples were subjected to ultracentrifugation. Afterward, 5 mL of 4% Ficoll buffer (2 mL of 10% Ficoll buffer and 3 mL of vacuole buffer) and 2 mL of vacuole buffer (0.45 M mannitol, 5 mM sodium phosphate, 2 mM EDTA; pH 7.5) were added by the use of standard 1-mL micropipette. The mixture was subsequently centrifuged in a compatible ultracentrifuge at 50,000 × g for 50 min at 10 °C. Vacuoles were detected at the 4% Ficoll buffer/vacuole buffer interface and collected using a standard 200-μL micropipette. The vacuoles were mixed with 7% nitric acid, after which elemental analysis was performed via ICP-MS.

Xylem sap collection

Seeds of Col-0 and *sec24c* were sown in soil and watered with Hoagland nutrient solution weekly. When they were 4 weeks old, the seedlings were exposed to 0 (control) or 20 μM Cd (treatment) for 4 days, after which xylem sap samples were then collected according to a previous method[43]. Briefly, stems were cut with a razor blade 2–3 cm above the basal stems to collect xylem sap during a 2-h period. Xylem sap collected during the first 10 min was discarded to avoid contamination from damaged cells. The xylem sap and 7% nitric acid were then mixed together, after which elemental analysis was performed via ICP-MS.

Protein interaction experiments

For the BiLC experiments, *Agrobacterium* (strain GV3101) harbouring the tested combinations was infiltrated into the leaves of *N. benthamiana*. The leaves were collected at 48 hours post-infiltration and then injected with 0.8 mM luciferin, after which the luciferase signals were captured using a Tanon 5200 system (a cooled charge-coupled device (CCD) imaging apparatus).

For Y2H assays, a DUAL membrane system (Clontech, Mountain View, CA, USA) was used according to the manufacturer's instructions. A pBT3-STE bait vector and a pPR3-N prey vector harbouring genes to be tested were co-transformed pairwise into *Saccharomyces cerevisiae* strain *NMY51*. A 10× dilution series of 10-μL aliquots of co-transformed *NMY51* was spotted onto SD-Trp-Leu-Ade-His selective plates. The plates were subsequently incubated at 30 °C for 3–5 days.

For BiFC experiments, leaf mesophyll protoplasts were prepared from the leaves of 14- to 21-day-old plants. Ten micrograms of plasmid DNA was transfected into protoplasts by transient expression according to the Arabidopsis mesophyll protoplast method. YFP fluorescence was observed with a Leica TCS SP8 confocal laser scanning microscope.

For Co-IP assays, *Agrobacterium*-mediated transient expression in *N. benthamiana* was used for protein expression. Protein samples were extracted with lysis buffer (P0013, Beyotime) and centrifuged at 15,000 rpm for 10 min. The protein extracts were then subjected to immunoprecipitation (IP) using anti-Myc beads. The input and bound proteins were analysed by electrophoresis on SDS–PAGE gels followed by

Western blot assays using anti-Myc or anti-Flag (BBI) antibodies. Immunoblots were detected using an ECL Western blotting substrate (Solarbio Science & Technology) and visualized using a Tanon 5200 digital imaging system (Tanon Science & Technology, Shanghai, China).

Chemical treatment

Stock solutions of various pharmacological drugs were prepared using dimethyl sulfoxide (DMSO) as the solvent at the following concentrations: 50 mM BFA, 115 μM ConcA and 4 mM FM4-64. Endocytosis and co-localization studies were performed with 4 μM FM4-64. Six-day-old seedlings were incubated in 1 mL of liquid media (1/2-strength MS media, 0.5% sucrose; pH 5.8) supplemented with FM4-64 (Invitrogen) for 15 min at room temperature. The seedlings were then washed three times with liquid 1/2-strength MS media and subsequently immersed in 50 μM BFA or 2 μM ConcA for 2 hours. The treated seedlings were then observed via confocal laser scanning microscopy (Leica TCS SP8).

Confocal microscopy

Confocal laser scanning microscopy was performed on a Leica TCS SP8 confocal microscope with the following spectral settings: excitation at 488 nm with an argon laser; emission at 498–550 nm for GFP, 565–600 nm for RFP, and 620–680 nm for FM4-64; and emission at 505–530 for the fluorescent signal of the Cd-sensitive dye. For the mCherry signal, the excitation wavelength was 561 nm, and the emission was 570–620 nm.

Declarations

Author contributions

D.Y.C. conceived the work, D.Y.C. and Q.Y.L. designed the experiments. Q.Y.L. performed most of the experiments. Y.Q.G., C.Y.Z., Z.F.C., L.Y.Z., Y.L.W. and M.L.H. performed some experiments. D.Y.C. and Q.Y.L. wrote the manuscript. All authors edited and commented on the manuscript

Acknowledgments

We would like to thank Professor Lin Xu for sharing the *pC131-YN* and *pC131-YC* vectors, and Professor Chaofeng Huang for the ST-mCherry vector. We are also appreciated for the seeds of T-DNA insertion lines and vectors of CD3-959-mCherry and CD3-975-mCherry from ABRC. This study was funded by the Ministry of Science and Technology Key R&D program (2016YFD0100700 to D.Y.C.), Chinese Academy of Sciences (XDB27010103 to D.Y.C), and the Natural Science Foundation of China (31930024 to D.Y.C).

References

1. Tan, X.; Li, K.; Wang, Z.; Zhu, K.; Tan, X.; Cao, J., A Review of Plant Vacuoles: Formation, Located Proteins, and Functions. *Plants (Basel)* 2019, *8* (9).
2. Bassham, D. C.; Brandizzi, F.; Otegui, M. S.; Sanderfoot, A. A., The secretory system of Arabidopsis. *Arabidopsis Book* 2008, *6*, e0116.
3. Pedrazzini, E.; Komarova, N. Y.; Rentsch, D.; Vitale, A., Traffic routes and signals for the tonoplast. *Traffic* 2013, *14* (6), 622–8.
4. Uemura, T.; Ueda, T., Plant vacuolar trafficking driven by RAB and SNARE proteins. *Curr Opin Plant Biol* 2014, *22*, 116–121.
5. Cui, Y.; Zhao, Q.; Gao, C.; Ding, Y.; Zeng, Y.; Ueda, T.; Nakano, A.; Jiang, L., Activation of the Rab7 GTPase by the MON1-CCZ1 Complex Is Essential for PVC-to-Vacuole Trafficking and Plant Growth in Arabidopsis. *Plant Cell* **2014**, *26* (5), 2080–2097.
6. Ebine, K.; Inoue, T.; Ito, J.; Ito, E.; Uemura, T.; Goh, T.; Abe, H.; Sato, K.; Nakano, A.; Ueda, T., Plant vacuolar trafficking occurs through distinctly regulated pathways. *Curr Biol* 2014, *24* (12), 1375–1382.
7. Singh, M. K.; Kruger, F.; Beckmann, H.; Brumm, S.; Vermeer, J. E. M.; Munnik, T.; Mayer, U.; Stierhof, Y. D.; Grefen, C.; Schumacher, K.; Jurgens, G., Protein delivery to vacuole requires SAND protein-dependent Rab GTPase conversion for MVB-vacuole fusion. *Curr Biol* 2014, *24* (12), 1383–1389.
8. Viotti, C.; Kruger, F.; Krebs, M.; Neubert, C.; Fink, F.; Lupanga, U.; Scheuring, D.; Boutte, Y.; Frescatada-Rosa, M.; Wolfenstetter, S.; Sauer, N.; Hillmer, S.; Grebe, M.; Schumacher, K., The endoplasmic reticulum is the main membrane source for biogenesis of the lytic vacuole in Arabidopsis. *Plant Cell* 2013, *25* (9), 3434–49.
9. Viotti, C., ER and vacuoles: never been closer. *Front Plant Sci* 2014, *5*, 20.
10. Stagg, S. M.; Gurkan, C.; Fowler, D. M.; LaPointe, P.; Foss, T. R.; Potter, C. S.; Carragher, B.; Balch, W. E., Structure of the Sec13/31 COPII coat cage. *Nature* 2006, *439* (7073), 234–8.
11. Stagg, S. M.; LaPointe, P.; Razvi, A.; Gurkan, C.; Potter, C. S.; Carragher, B.; Balch, W. E., Structural basis for cargo regulation of COPII coat assembly. *Cell* 2008, *134* (3), 474–84.
12. Zanetti, G.; Prinz, S.; Daum, S.; Meister, A.; Schekman, R.; Bacia, K.; Briggs, J. A., The structure of the COPII transport-vesicle coat assembled on membranes. *Elife* 2013, *2*, e00951.
13. Faso, C.; Chen, Y. N.; Tamura, K.; Held, M.; Zemelis, S.; Marti, L.; Saravanan, R.; Hummel, E.; Kung, L.; Miller, E.; Hawes, C.; Brandizzi, F., A missense mutation in the Arabidopsis COPII coat protein Sec24A induces the formation of clusters of the endoplasmic reticulum and Golgi apparatus. *Plant Cell* 2009, *21* (11), 3655–71.
14. Nakano, R. T.; Matsushima, R.; Ueda, H.; Tamura, K.; Shimada, T.; Li, L.; Hayashi, Y.; Kondo, M.; Nishimura, M.; Hara-Nishimura, I., GNOM-LIKE1/ERMO1 and SEC24a/ERMO2 are required for maintenance of endoplasmic reticulum morphology in Arabidopsis thaliana. *Plant Cell* **2009**, *21* (11), 3672–85.
15. Tanaka, Y.; Nishimura, K.; Kawamukai, M.; Oshima, A.; Nakagawa, T., Redundant function of two Arabidopsis COPII components, AtSec24B and AtSec24C, is essential for male and female

gametogenesis. *Planta* 2013, *238* (3), 561–75.

16. Morel, M.; Crouzet, J.; Gravot, A.; Auroy, P.; Leonhardt, N.; Vavasseur, A.; Richaud, P., AtHMA3, a P1B-ATPase allowing Cd/Zn/Co/Pb vacuolar storage in Arabidopsis. *Plant Physiol* **2009**, *149* (2), 894–904.
17. Thomine, S.; Wang, R.; Ward, J. M.; Crawford, N. M.; Schroeder, J. I., Cadmium and iron transport by members of a plant metal transporter family in Arabidopsis with homology to Nramp genes. *Proc Natl Acad Sci U S A* 2000, *97* (9), 4991–6.
18. Oomen, R. J.; Wu, J.; Lelievre, F.; Blanchet, S.; Richaud, P.; Barbier-Brygoo, H.; Aarts, M. G.; Thomine, S., Functional characterization of NRAMP3 and NRAMP4 from the metal hyperaccumulator Thlaspi caerulescens. *New Phytol* **2009**, *181* (3), 637–50.
19. Rea, P. A., Plant ATP-binding cassette transporters. *Annu Rev Plant Biol* 2007, *58*, 347–75.
20. Liu, G.; Sanchez-Fernandez, R.; Li, Z. S.; Rea, P. A., Enhanced multispecificity of arabidopsis vacuolar multidrug resistance-associated protein-type ATP-binding cassette transporter, AtMRP2. *J Biol Chem* 2001, *276* (12), 8648–56.
21. Song, W. Y.; Park, J.; Mendoza-Cozatl, D. G.; Suter-Grotemeyer, M.; Shim, D.; Hortensteiner, S.; Geisler, M.; Weder, B.; Rea, P. A.; Rentsch, D.; Schroeder, J. I.; Lee, Y.; Martinoia, E., Arsenic tolerance in Arabidopsis is mediated by two ABCC-type phytochelatin transporters. *Proc Natl Acad Sci U S A* 2010, *107* (49), 21187–92.
22. Park, J.; Song, W. Y.; Ko, D.; Eom, Y.; Hansen, T. H.; Schiller, M.; Lee, T. G.; Martinoia, E.; Lee, Y., The phytochelatin transporters AtABCC1 and AtABCC2 mediate tolerance to cadmium and mercury. *Plant J* 2012, *69* (2), 278–88.
23. Adolf, F.; Rhiel, M.; Reckmann, I.; Wieland, F. T., Sec24C/D-isoform-specific sorting of the preassembled ER-Golgi Q-SNARE complex. *Mol Biol Cell* **2016**, *27* (17), 2697–707.
24. Mancias, J. D.; Goldberg, J., Structural basis of cargo membrane protein discrimination by the human COPII coat machinery. *Embo Journal* 2008, *27* (21), 2918–2928.
25. Pedrazzini, E.; Komarova, N. Y.; Rentsch, D.; Vitale, A., Traffic Routes and Signals for the Tonoplast. *Traffic* 2013, *14* (6), 622–628.
26. Hanton, S. L.; Chatre, L.; Renna, L.; Matheson, L. A.; Brandizzi, F., De novo formation of plant endoplasmic reticulum export sites is membrane cargo induced and signal mediated. *Plant Physiol* 2007, *143* (4), 1640–50.
27. Bottanelli, F.; Foresti, O.; Hanton, S.; Denecke, J., Vacuolar transport in tobacco leaf epidermis cells involves a single route for soluble cargo and multiple routes for membrane cargo. *Plant Cell* 2011, *23* (8), 3007–25.
28. Geldner, N.; Anders, N.; Wolters, H.; Keicher, J.; Kornberger, W.; Muller, P.; Delbarre, A.; Ueda, T.; Nakano, A.; Jurgens, G., The Arabidopsis GNOM ARF-GEF mediates endosomal recycling, auxin transport, and auxin-dependent plant growth. *Cell* 2003, *112* (2), 219–30.
29. Dettmer, J.; Hong-Hermesdorf, A.; Stierhof, Y. D.; Schumacher, K., Vacuolar H+-ATPase activity is required for endocytic and secretory trafficking in Arabidopsis. *Plant Cell* 2006, *18* (3), 715–30.

30. Viotti, C.; Krueger, F.; Krebs, M.; Neubert, C.; Fink, F.; Lupanga, U.; Scheuring, D.; Boutte, Y.; Frescatada-Rosa, M.; Wolfenstetter, S.; Sauer, N.; Hillmer, S.; Grebe, M.; Schumacher, K., The Endoplasmic Reticulum Is the Main Membrane Source for Biogenesis of the Lytic Vacuole in Arabidopsis. *Plant Cell* 2013, *25* (9), 3434–3449.
31. Sohn, E. J.; Kim, E. S.; Zhao, M.; Kim, S. J.; Kim, H.; Kim, Y. W.; Lee, Y. J.; Hillmer, S.; Sohn, U.; Jiang, L.; Hwang, I., Rha1, an Arabidopsis Rab5 homolog, plays a critical role in the vacuolar trafficking of soluble cargo proteins. *Plant Cell* 2003, *15* (5), 1057–70.
32. Lee, G. J.; Sohn, E. J.; Lee, M. H.; Hwang, I., The Arabidopsis Rab5 homologs Rha1 and Ara7 localize to the prevacuolar compartment. *Plant and Cell Physiology* 2004, *45* (9), 1211–1220.
33. Cui, Y.; Zhao, Q.; Hu, S.; Jiang, L., Vacuole Biogenesis in Plants: How Many Vacuoles, How Many Models? *Trends Plant Sci* **2020**, *25* (6), 538–548.
34. Wang, J.; Sun, P.; Li, Y.; Liu, Y.; Yang, N.; Yu, J.; Ma, X.; Sun, S.; Xia, R.; Liu, X.; Ge, D.; Luo, S.; Liu, Y.; Kong, Y.; Cui, X.; Lei, T.; Wang, L.; Wang, Z.; Ge, W.; Zhang, L.; Song, X.; Yuan, M.; Guo, D.; Jin, D.; Chen, W.; Pan, Y.; Liu, T.; Yang, G.; Xiao, Y.; Sun, J.; Zhang, C.; Li, Z.; Xu, H.; Duan, X.; Shen, S.; Zhang, Z.; Huang, S.; Wang, X., An Overlooked Paleotetraploidization in Cucurbitaceae. *Mol Biol Evol* 2018, *35* (1), 16–26.
35. Uemura, T.; Ueda, T., Plant vacuolar trafficking driven by RAB and SNARE proteins. *Current Opinion in Plant Biology* 2014, *22*, 116–121.
36. Chung, K. P.; Zeng, Y.; Jiang, L., COPII Paralogs in Plants: Functional Redundancy or Diversity? *Trends Plant Sci* 2016, *21* (9), 758–769.
37. Gao, Y. Q.; Chen, J. G.; Chen, Z. R.; An, D.; Lv, Q. Y.; Han, M. L.; Wang, Y. L.; Salt, D. E.; Chao, D. Y., A new vesicle trafficking regulator CTL1 plays a crucial role in ion homeostasis. *PLoS Biol* **2017**, *15* (12), e2002978.
38. Chao, D. Y.; Chen, Y.; Chen, J.; Shi, S.; Chen, Z.; Wang, C.; Danku, J. M.; Zhao, F. J.; Salt, D. E., Genome-wide association mapping identifies a new arsenate reductase enzyme critical for limiting arsenic accumulation in plants. *PLoS Biol* 2014, *12* (12), e1002009.
39. Cailliatte, R.; Schikora, A.; Briat, J. F.; Mari, S.; Curie, C., High-affinity manganese uptake by the metal transporter NRAMP1 is essential for Arabidopsis growth in low manganese conditions. *Plant Cell* 2010, *22* (3), 904–17.
40. Gou, J. Y.; Felippes, F. F.; Liu, C. J.; Weigel, D.; Wang, J. W., Negative regulation of anthocyanin biosynthesis in Arabidopsis by a miR156-targeted SPL transcription factor. *Plant Cell* 2011, *23* (4), 1512–22.
41. Lahner, B.; Gong, J.; Mahmoudian, M.; Smith, E. L.; Abid, K. B.; Rogers, E. E.; Guerinot, M. L.; Harper, J. F.; Ward, J. M.; McIntyre, L.; Schroeder, J. I.; Salt, D. E., Genomic scale profiling of nutrient and trace elements in Arabidopsis thaliana. *Nat Biotechnol* 2003, *21* (10), 1215–21.
42. Schneider, S.; Hulpke, S.; Schulz, A.; Yaron, I.; Holl, J.; Imlau, A.; Schmitt, B.; Batz, S.; Wolf, S.; Hedrich, R.; Sauer, N., Vacuoles release sucrose via tonoplast-localised SUC4-type transporters. *Plant Biol (Stuttg)* 2012, *14* (2), 325–36.

43. Ceballos-Laita, L.; Gutierrez-Carbonell, E.; Takahashi, D.; Abadia, A.; Uemura, M.; Abadia, J.; Lopez-Millan, A. F., Effects of Fe and Mn deficiencies on the protein profiles of tomato (Solanum lycopersicum) xylem sap as revealed by shotgun analyses. *J Proteomics* 2018, *170*, 117–129.

Figures

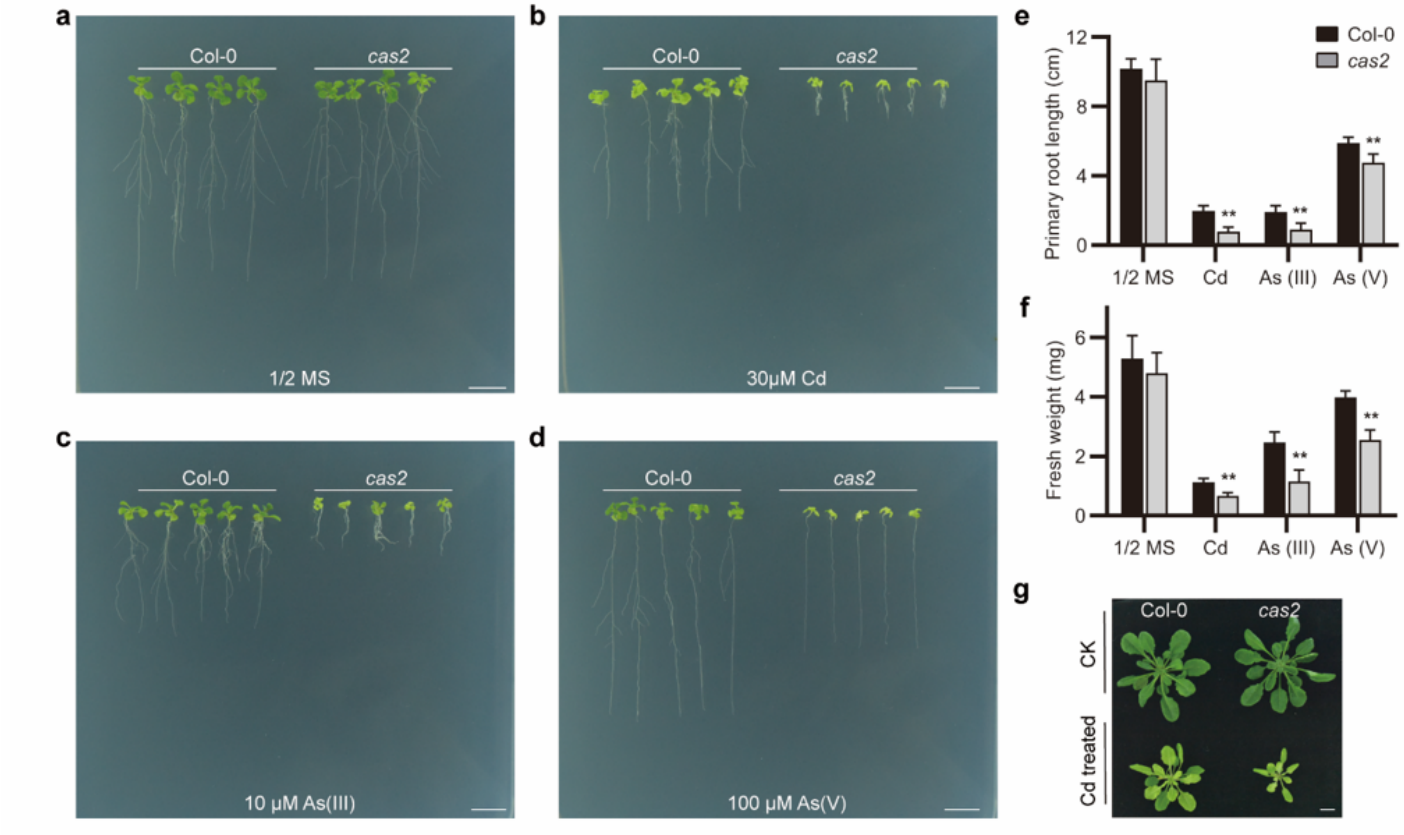

Figure 1

Phenotypes of the mutant cadmium-sensitive and arsenic-sensitive 2 (cas2). a-d, A. thaliana wild-type (Col-0) and cas2 mutant seedlings grown on half-strength MS media in the absence (a) or presence of 30 μM CdCl2 (b), 10 μM As(III) (c), or 100 μM As(V) (d) for 14 days. e-f, Comparison of Cd and As tolerance between the wild-type and cas2 mutant seedlings based on fresh weight (e) and primary root length (f). The values are the means ± SDs (n = 21–48 for the fresh weight analysis, and n = 11–30 for primary root length measurements). **, P<0.01 (two-tailed paired Student's t-test). g, Col-0 and cas2 grown for 3 weeks under normal hydroponic conditions followed by exposure to 0 (CK) or 20 μM CdCl2 (Cd-treated) for 4 days. Scale bars, 1 cm.

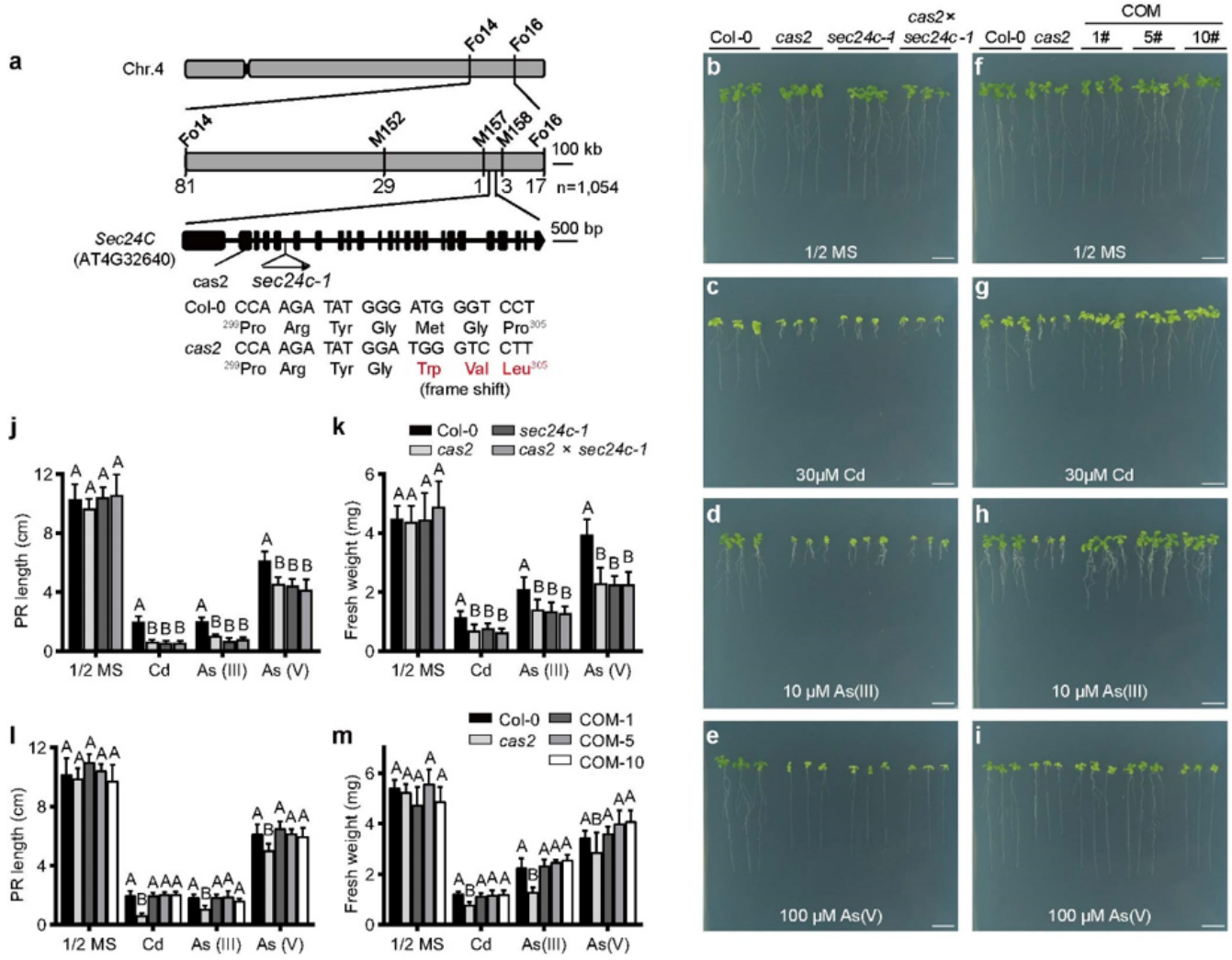

Figure 2

Map-based cloning and complementation of cas2. a, Mapping of cas2, in which 1,054 F2 plants were used to narrow the location of the candidate gene to a 100-kb region between markers M157 and M158. The numbers under the markers are the number of recombinants between the causal gene and the indicated marker. The gene structure of Sec24C and the mutation in cas2 and sec24c-1 are shown at the bottom. b-i, Two-week-old Col-0, cas2, sec24c-1, cas2 × sec24c-1 F1 (b-e), and three complementation lines (com 1#, 5# and 10#) (f-i) grown on media without heavy metals (b,f) or with 30 μM CdCl2 (c, g), 10 μM As(III) (d,h), or 100 μM As(V) (e, i). j-k, Statistical analysis of the primary root length (j) and fresh weight (k) of each genotype in b-e. l-m, Statistical analysis of the primary root length (l) and fresh weight (m) of seedlings in f-i. The values are shown as the means ± SDs (n = 15–45 for primary root length measurements, and n = 18–48 for fresh weight analysis). The different letters above the bars indicate significant differences at $P < 0.01$ (one-way ANOVA with Tukey's HSD test). Scale bars, 1 cm.

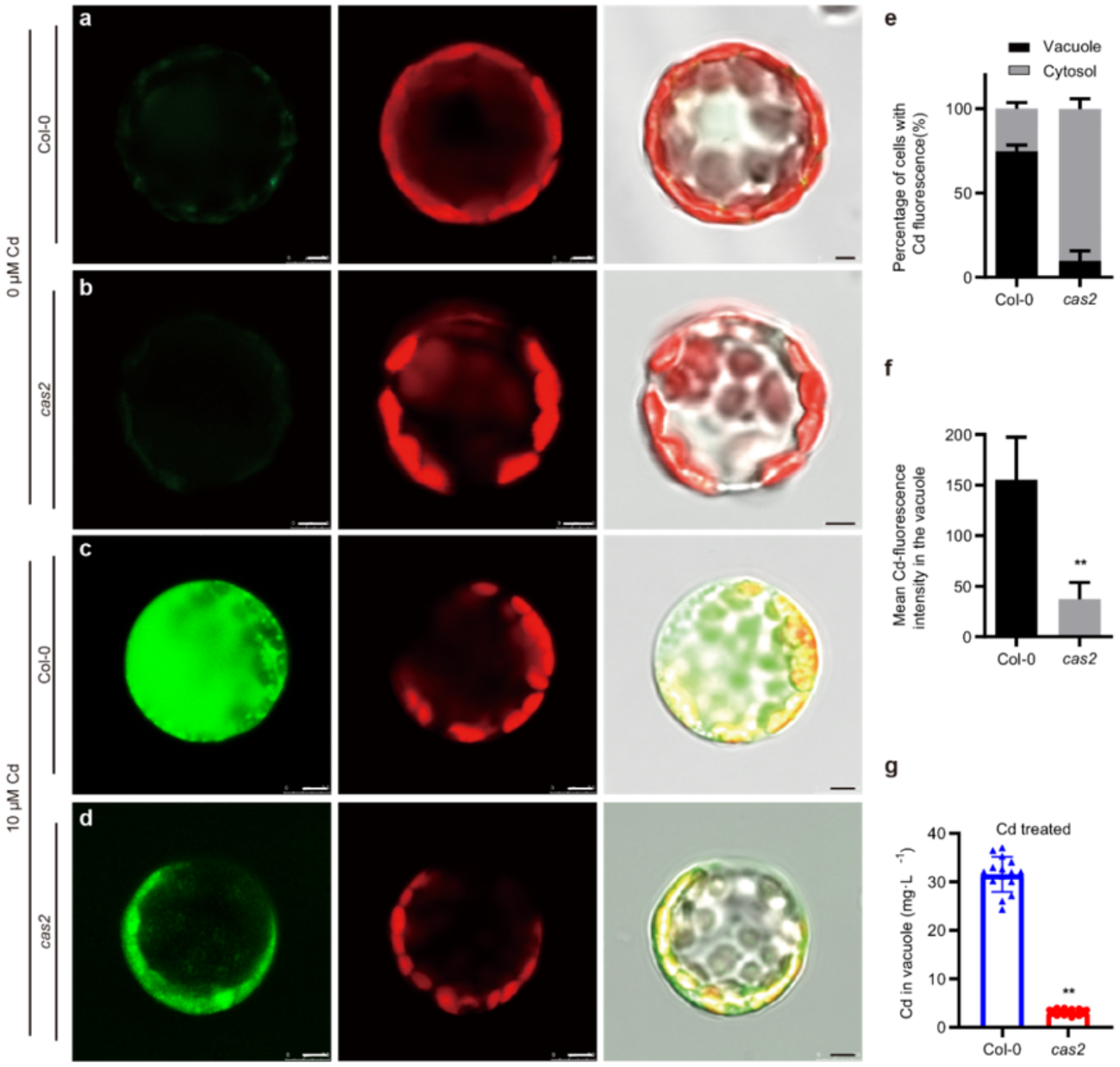

Figure 3

Loss function of Sec24C impairs Cd compartmentalization in vacuoles. a-d, Protoplasts of 2-week-old Col-0 (a, c) and cas2 (b,d) plants stained with the Cd indicator LeadmiumTM Green. The seedlings were grown on 1/2-strength MS media (a,b) or 1/2-strength MS media containing 10 μM CdCl2 (c,d). The green channel shows LeadmiumTM Green-derived Cd fluorescence (left panels), the red channel shows chlorophyll autofluorescence (middle panels), and merged bright field images are shown in the right panels. The images were captured under the same laser intensity. e, Percentage of cells exhibiting vacuolar or cytosolic patterns of Cd fluorescence in c-d. The data represent the means ± SDs (n = 5–7). f, Fluorescence signal intensity of the vacuoles in c-d. The data represent the means ± SDs (n = 23). g, Cd content in isolated vacuoles of Col-0 and cas2 plants. The plants were grown in normal hydroponic

culture for 3 weeks and then treated with 20 μM CdCl2 for 4 days. n = 15. The data represent the means ± SDs. **, P< 0.01 (two-tailed paired Student's t-test). Scale bars, 5 μm.

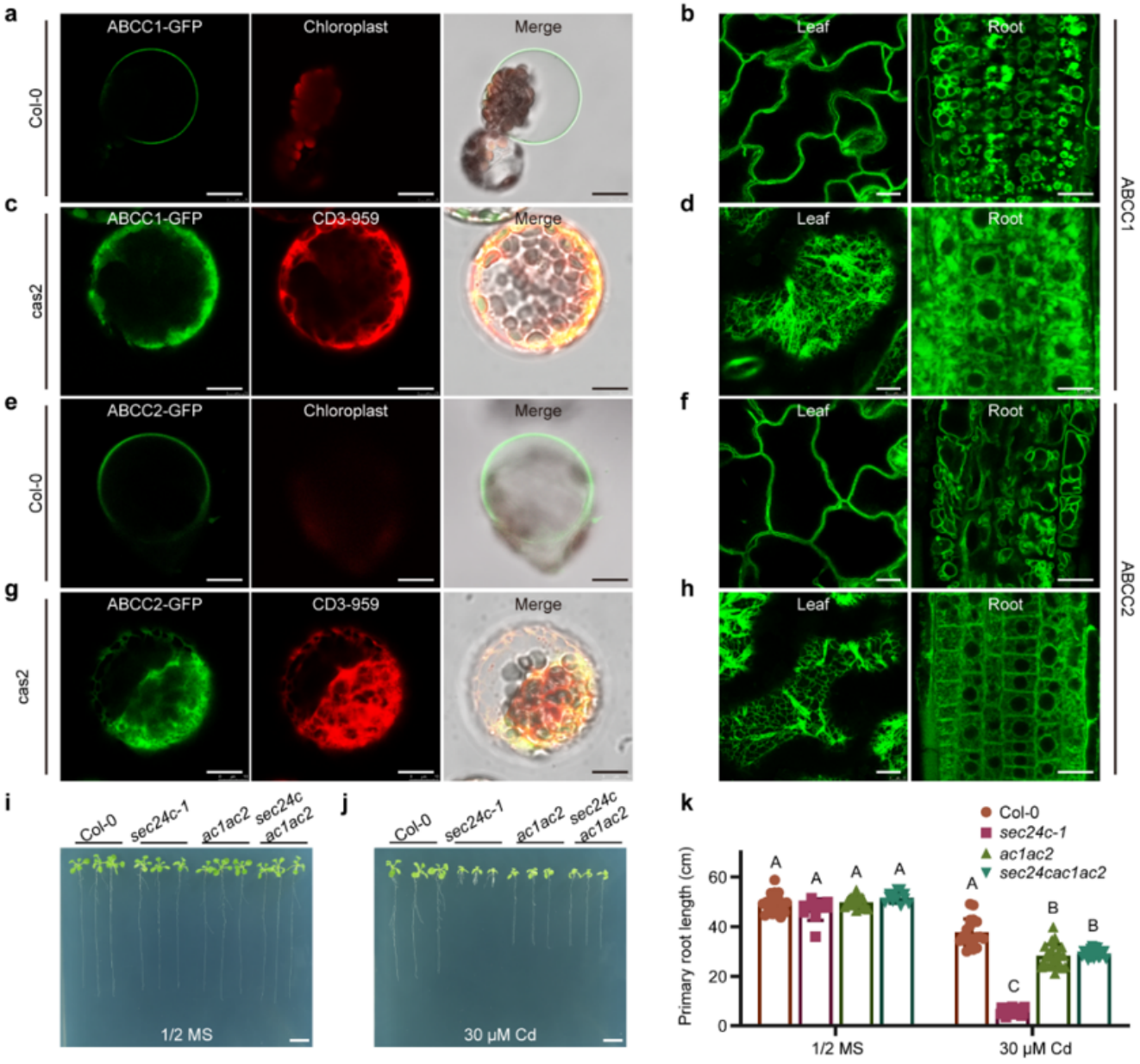

Figure 4

Sec24C is required for tonoplast localization of the phytochelatin transporters ABCC1 and ABCC2. a-d, Subcellular localization of ABCC1 in protoplasts (a,c), or cells of leaves and roots (b,d) of Col-0 (a,b) and cas2 (c,d). e-h, Subcellular localization of ABCC2 in protoplasts (e, g), or cells of leaves and roots (f,h) of Col-0 (e,f) and cas2 (g,h). In a,e, the protoplasts were osmotically lysed to show vacuoles. In c,g, the red channel shows the ER marker CD3-959. i,j, Phenotype of 2-week-old Col-0, sec24c-1, abcc1/abcc2 (ac1ac2) double mutant, and sec24c-1/abcc1/abcc2 triple mutant (sec24cac1ac2) plants grown on 1/2-strength MS media only (i) or 1/2-strength MS media supplemented with 30 μM CdCl2 (j). k, Statistical analysis of the primary root length of seedlings shown in i-j. Data represent the means ± SDs (n = 10–

25). Different letters indicate a significant difference (P< 0.01) using Tukey's HSD test. Bars, 10 μm (a-h), 10 mm (i,j).

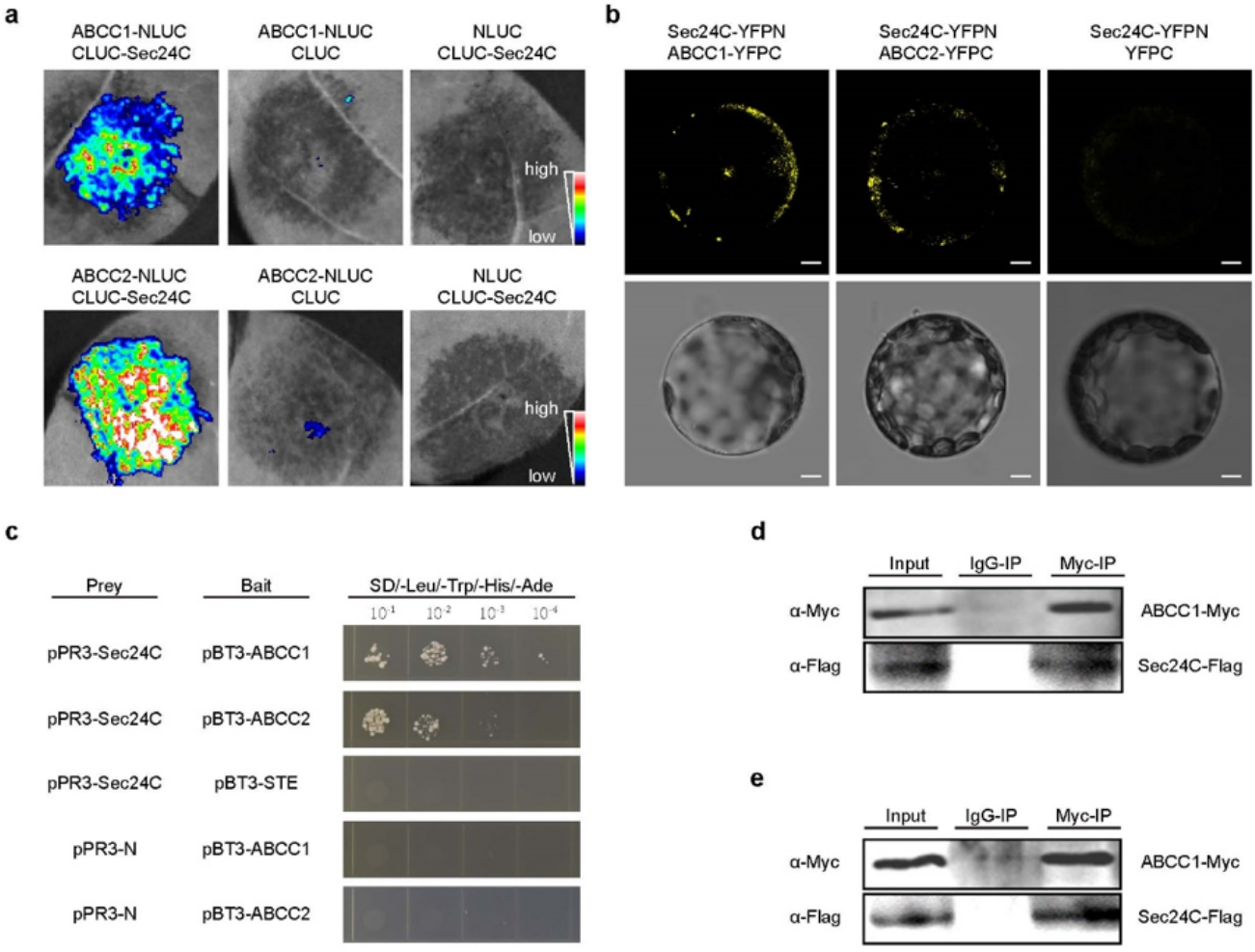

Figure 5

Sec24C physically interacts with ABCC1 and ABCC2. a, BiLC experiments performed in N. benthamiana leaves. The fluorescence signal intensities represent the interaction strength between Sec24C and ABCC1 or ABCC2 (as indicated). b, BiFC assays. A. thaliana protoplasts were co-transformed with the constructs indicated and were imaged using a confocal microscope after incubation at room temperature for 18 hours. YFP fluorescence indicates the protein–protein interaction. The combination of Sec24C-YFPN and YFPC was used as a negative control. c, Membrane-based Y2H experiment detecting the interactions between Sec24C and ABCC1 or ABCC2. Cells of yeast strain NMY51 co-transformed with bait and prey vectors (as indicated) were grown on high-stringency selective media (SD/-Leu/-Trp/-His/-Ade). d,e, Co-IP experiments to detect the interactions between Sec24C and ABCC1 (d) or ABCC2 (e). Scale bar, 5 μm.

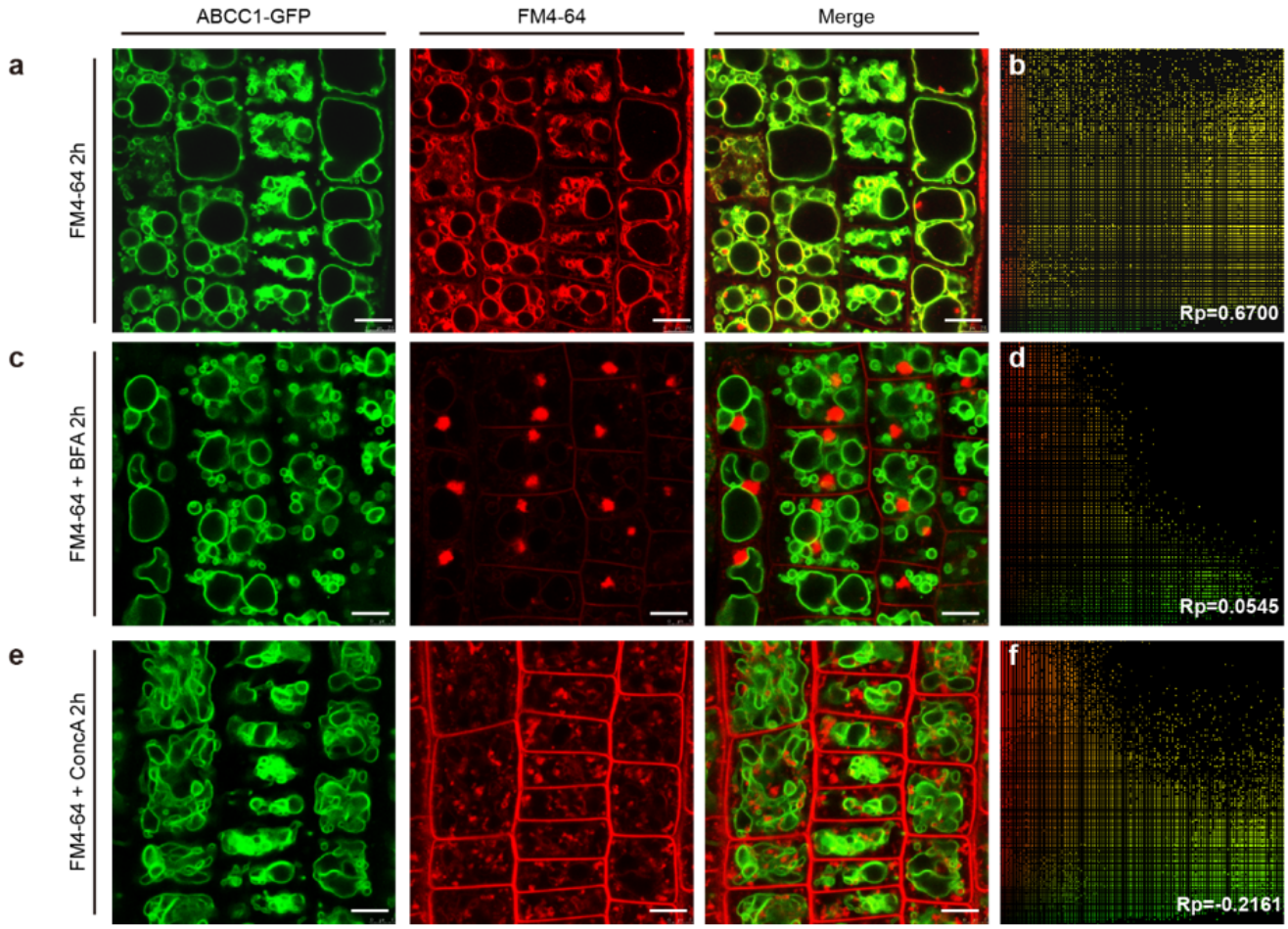

Figure 6

Tonoplast localization of ABCC1 is independent of the Golgi and TGN/EE. a,b, Confocal laser scanning micrograph of root epidermal cells from 6-day-old seedlings of ABCC1-GFP transgenic plants treated with FM4-64 for 15 min and observed after 2 h of incubation in 1/2-strength MS. c-f, ABCC1-GFP- or FM4-64-derived signal in root epidermal cells treated with FM4-64 for 15 min followed by an incubation in BFA (c,d) or ConcA (e,f) for 2h. The green channel shows the GFP signal (left panels), the red channel shows the FM4-64 signal (middle panels) and the merged images are shown in the right panels. In b,d,f, Pearson correlation coefficient (Rp) analysis of the green and red signals in a,c, and e, respectively. Scale bar, 10 µm.

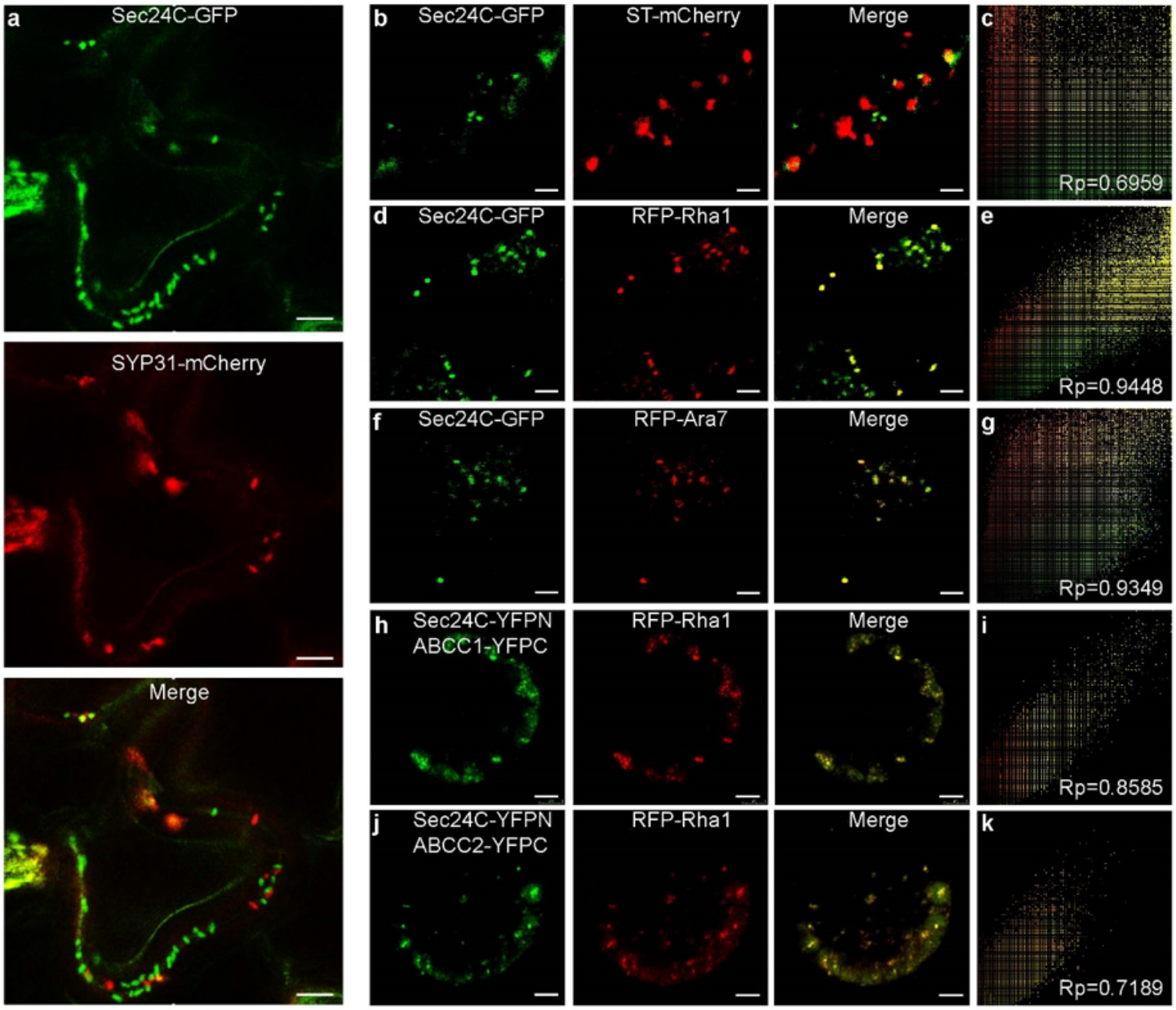

Figure 7

Sec24C mediates PVC localization of ABCC1 and ABCC2. a-g, Co-localization analysis of Sec24C with the Golgi markers SYP31-mCherry (a) and ST-mCherry (b,c) and the PVC markers RFP-Rha1 (d,e) and RFP-Ara7 (f,g) in A. thaliana leaf epidermal cells (a) or protoplasts derived from A. thaliana mesophyll cells (b-g). h-k, Co-localization analysis of the complexes of Sec24C-ABCC1 (h,i) and Sec24C-ABCC2 (j,k) with the PVC marker RFP-Rha1. In b,d,f,h,j, images of GFP or YFP fluorescence (left), mCherry or RFP fluorescence (centre) and the merged images (right) are shown. c,e,g,i,k, Pearson correlation coefficient (Rp) analysis of the green and red signals in b,d,f,h and j, respectively. Scale bars, 1 μm (b,d,f), 5 μm (a,h,j).

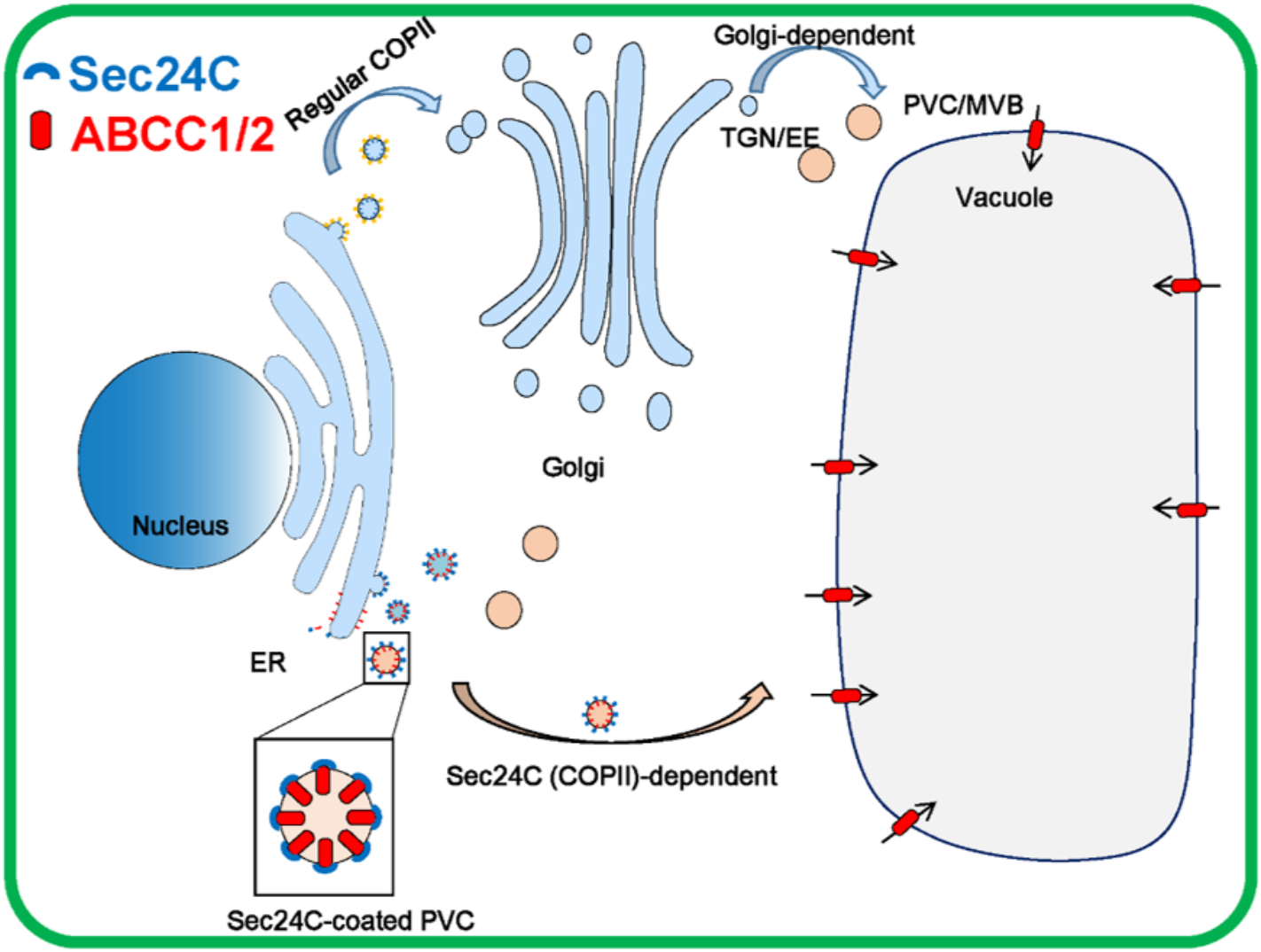

Figure 8

Proposed Sec24C-mediated cargo trafficking pathway from the ER to the vacuole. The classic vacuolar trafficking route utilizes COPII-mediated anterograde trafficking from the ER to the Golgi and involves passing through the TGN/EE to PVCs/MVBs, after which the vacuole is ultimately reached. In this Sec24C-mediated trafficking route model, ABCC1 and ABCC2 are selectively packed into Sec24C-dependent COPII vesicles at the ER and destined for PVCs directly through a Golgi-independent trafficking pathway, ultimately targeting the tonoplast. The function of Sec24C is essential for correct targeting of ABCC1 and ABCC2 to the tonoplast and confers heavy metal resistance to A. thaliana.

Supplementary Files

This is a list of supplementary files associated with this preprint. Click to download.

- supplementaryfigures.pdf

- SupplementaryTable1.docx